

Are small-scale sub-structures a universal property of galaxy halos? The case of the giant elliptical NGC 5128

M. Mouhcine¹, R. Ibata², M. Rejkuba³

¹ *Astrophysics Research Institute, Liverpool John Moores University, Twelve Quays House, Egerton Wharf, Birkenhead, CH41 1LD, UK*

² *Observatoire Astronomique de Strasbourg (UMR 7550), 11, rue de l'Université, 67000 Strasbourg, France*

³ *ESO, Karl-Schwarzschild-Strasse 2, D-85748 Garching, Germany*

16 November 2018

ABSTRACT

We present an analysis of the spatial and chemical sub-structures in a remote halo field in the nearby giant elliptical galaxy Centaurus A (NGC 5128), situated ~ 38 kpc from the centre of the galaxy. The observations were taken with the Advanced Camera for Surveys instrument on board the Hubble Space Telescope, and reach down to the horizontal branch. In this relatively small $3.8 \text{ kpc} \times 3.8 \text{ kpc}$ field, after correcting for Poisson noise, we do not find any statistically strong evidence for the presence of small-scale sub-structures in the stellar spatial distribution on scales $\gtrsim 100 \text{ pc}$. However, we do detect the presence of significant small spatial-scale inhomogeneities in the stellar median metallicity over the surveyed field. We argue that these localized chemical substructures could be associated with not-fully mixed debris from the disruption of low mass systems. NGC 5128 joins the ranks of the late-type spiral galaxies the Milky Way, for which the stellar halo appears to be dominated by small-scale spatial sub-structures, and NGC 891, where localized metallicity variations have been detected in the inner extra-planar regions. This suggests that the presence of small-scale sub-structures may be a generic property of stellar halos of large galaxies.

Key words: galaxies: formation – galaxies: stellar content – galaxies: individual (NGC 5128) – galaxies: haloes

1 INTRODUCTION

The early history of galaxy assembly leaves its signatures in the properties of the stellar content of the outer regions of galaxies. The currently-favored scenario of galaxy formation in a hierarchical context predicts that the vast majority of stars in the outskirts of galaxies should be accreted from disrupted satellite galaxies (e.g. Abadi et al. 2006; Zolotov et al. 2009). The ages, metallicities, spatial distribution, and amount of sub-structures in the faint outskirts of present-day galaxies are therefore directly related to their assembly histories, and to issues such as the suppression of star formation in small halos.

Recent wide field observations of the Milky Way have led to the identification of a number of large-scale stellar features, attributed either to past accretion of identified satellites (e.g. Ibata et al. 1994; Yanny et al. 2000, 2003; Newberg et al. 2002; Majewski et al. 2002), others

of unknown progenitors (e.g. Grillmair & Dionatos 2006; Belokurov et al. 2007), and others to the disruption of globular clusters (e.g. Odenkirchen et al. 2001; Grillmair 2009). The accretion of stars from satellites is clearly a contributor to the stellar haloes of galaxies. Quantitative analysis of wide-field imaging data from the Sloan Digital Sky Survey indicates that the stellar halo of the Milky Way is highly structured on small scales (Bell et al. 2008).

For the nearest Milky Way analogue NGC 891, the analysis of deep and high resolution imaging data sampling a quadrant running parallel to the high surface brightness disk of the galaxy, and extending outward to more than 10 kpc from the plane of the galaxy, identified strong evidence for the presence of highly significant small-scale substructures in the median metallicity map (Ibata et al. 2009). The degree of substructures present on the stellar density distribution in the halo of NGC 891 is found to be strikingly comparable to what is present in the Milky Way (Ibata et al. 2009). The extra-planar regions of NGC 891 appear to be composed of a large number of incompletely-mixed sub-populations. The discovery of a giant stream that loops around the galaxy and a series of low surface brightness features in its out-

¹ This work was based on observations with the NASA/ESA Hubble Space Telescope, obtained at the Space Telescope Science Institute, which is operated by the Association of Universities for Research in Astronomy, Inc., under NASA contract NAS 5-26555.

skirts demonstrates that NGC 891 had an active accretion history (Mouhcine et al. 2010a).

Being the nearest giant elliptical galaxy, NGC 5128 and its outer regions in particular have been targeted extensively as a unique testing ground for stellar population and formation models of elliptical galaxies (Soria et al. 1996; Harris et al. 1999; Marleau et al. 2000; Harris & Harris 2000, 2002; Rejkuba et al. 2001, 2002, 2005). The colour-magnitude diagrams of the stellar populations in the remote regions of the galaxy suggest that those regions are dominated by moderately metal-rich stars, i.e., $[M/H] \sim -0.65$, with a very wide red giant branch, suggesting that stars at large radii span a wide range of metallicities (Harris et al. 1999; Harris & Harris 2002). Different stellar age indicators, i.e., the red clump, the asymptotic giant branch bump, the period distribution of long period variables, globular clusters, suggest that the outer regions of NGC 5128 are populated by old stars, with a likely presence of a small fraction of intermediate age stars (Soria et al. 1996; Rejkuba et al. 2001, 2003; Woodley et al. 2010).

Possible formation histories of elliptical galaxies come generically in three flavours, first an early and rapid in-situ formation (e.g. Larson 1974; Harris et al 1995), secondly later mergers of pre-existing disk galaxies (e.g. Toomre 1977; Ashman & Zepf 1992), and finally as the results of multiple dissipationless mergers and accretions of distinct protogalactic fragments (e.g. Côté et al. 1998). Significant effort has been devoted over the years to test these scenarios using a variety of discriminants, e.g. stellar ages, chemical abundances, kinematics, and globular cluster systems. These different formation histories should give rise also to different stellar halo structures. The in-situ formation would predict relatively few substructures, as the formation epoch was many dynamical times ago. The stellar halos of elliptical galaxies that have grown hierarchically through mergers and accretions would be however substantially lumpy, and possibly as structured as those predicted by the most extreme cold-dark matter hierarchical formation models.

The purpose of the present paper is to examine the distribution of the stellar populations in the outer regions of NGC 5128, and to investigate in particular the clumpiness of the spatial and chemical structure of the halo population of a giant early-type galaxy for the first time. The data upon which this study is based have been presented in detail in Rejkuba et al. (2005, hereafter referred to as R05). The layout of this paper is as follows: in §2 we briefly introduce the data set used in the paper, while §3 presents the analysis to uncover small-scale sub-structures over the surveyed area. The implications of our findings are discussed in §4, and we draw our conclusions in §5.

Throughout this paper we assume a distance of 3.8 Mpc, i.e., distance modulus of $(m - M)_0 = 27.92$ (Rejkuba et al. 2005; Harris et al. 2009). We note that NGC 5128 is located at relatively low Galactic latitude ($\ell = 309.52^\circ$, $b = 19.42^\circ$), and therefore the targeted field suffers from significant (though not large) extinction from foreground dust. Following R05, we adopt a reddening value of $E(B - V) = 0.11$ (Burstein & Heiles 1982; Schlegel et al. 1998), which corresponds approximately to $A_V = 0.36$ and $A_I = 0.21$.

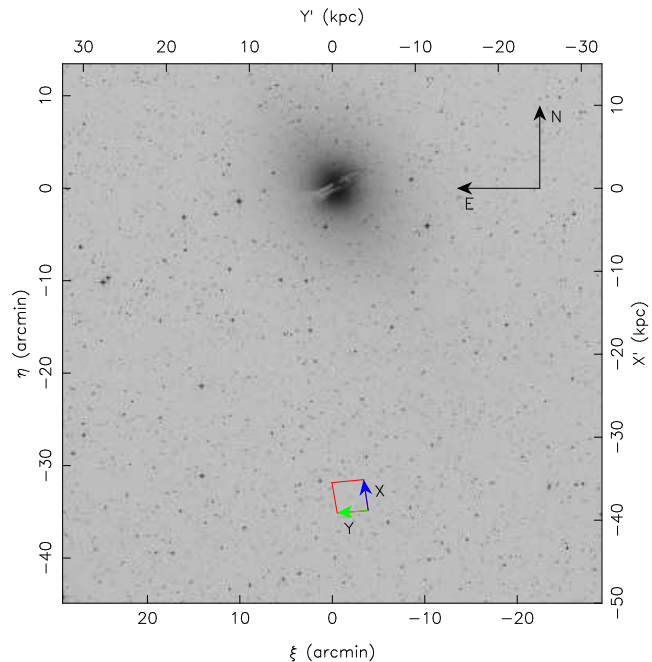


Figure 1. The location of the ACS field studied in this contribution lies ~ 38 kpc to the South of NGC 5128, superimposed on a photographic image extracted from the Digitized Sky Survey. The scale of the region is shown both in arcmin and kpc at the distance of NGC 5128. The X and Y axes of the ACS mosaic, as constructed by Rejkuba et al. (2005) are displayed on the image; these correspond approximately to the directions North and East, respectively.

2 DATA

As described in detail in R05, a single deep pointing was observed with the Advanced Camera for Surveys (ACS) camera on-board the Hubble Space Telescope (HST) in the halo of the galaxy NGC 5128 (program GO-9373), at a location approximately ~ 38 kpc South of the nucleus (Fig. 1). The target field was chosen to avoid any peculiarities of the galaxy, such as jet-induced star-forming regions (Mould et al. 2000; Rejkuba et al. 2002), shells (Malin et al. 1983), and dust lanes (Stickel et al. 2004). The F606W and F814W passbands were used (approximately broad-band Johnson V and Kron-Cousins I), with a total exposure of 8.58 hr (12 full-orbits) in each filter, which reaches $F606W \sim 30$, $F814W \sim 29$. ALLFRAME software (Stetson 1994) has been used to measure the photometry of all detected sources on the ACS images. To select stellar objects, we applied the criteria of R05 (summarised in their Fig. 3), namely those sources with ALLFRAME sharpness parameter within their defined hyperbolic envelope, and with chi-squared < 3 . The left panel of figure 2 shows the foreground reddening-corrected colour-magnitude diagram (CMD) of all objects detected in our images and classified as stars in the deep ACS halo field. The CMD are shown as density contours to reveal features in otherwise crowded regions. In addition to the wide sequence of red giant stars, red clump stars are visible at $I_o \sim 27.5$ and $(V - I)_o \sim 1.0$, and those on the AGB bump at $I_o \sim 26.5$ and $(V - I)_o \sim 1.3$.

Careful analysis of the completeness corrections and photometric uncertainties has been conducted via Monte-

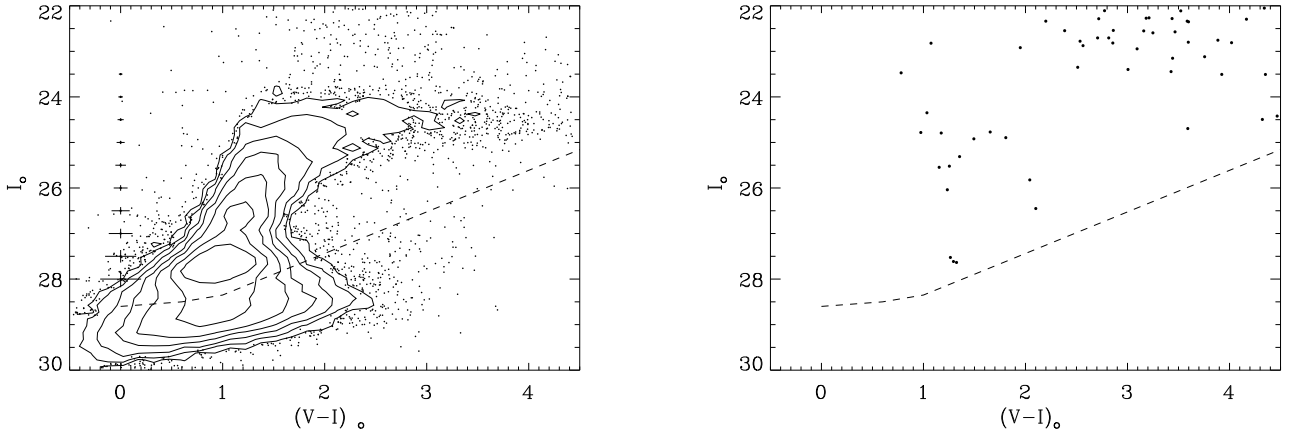


Figure 2. The left panel shows the foreground reddening-corrected colour-magnitude diagram of the targeted halo field. The dashed line shows the 50% detection completeness level. The right panel shows the colour-magnitude diagram of foreground stars as predicted by the Besançon Galactic population model in the direction of NGC 5128 over the same field-of-view as covered with a single ACS pointing.

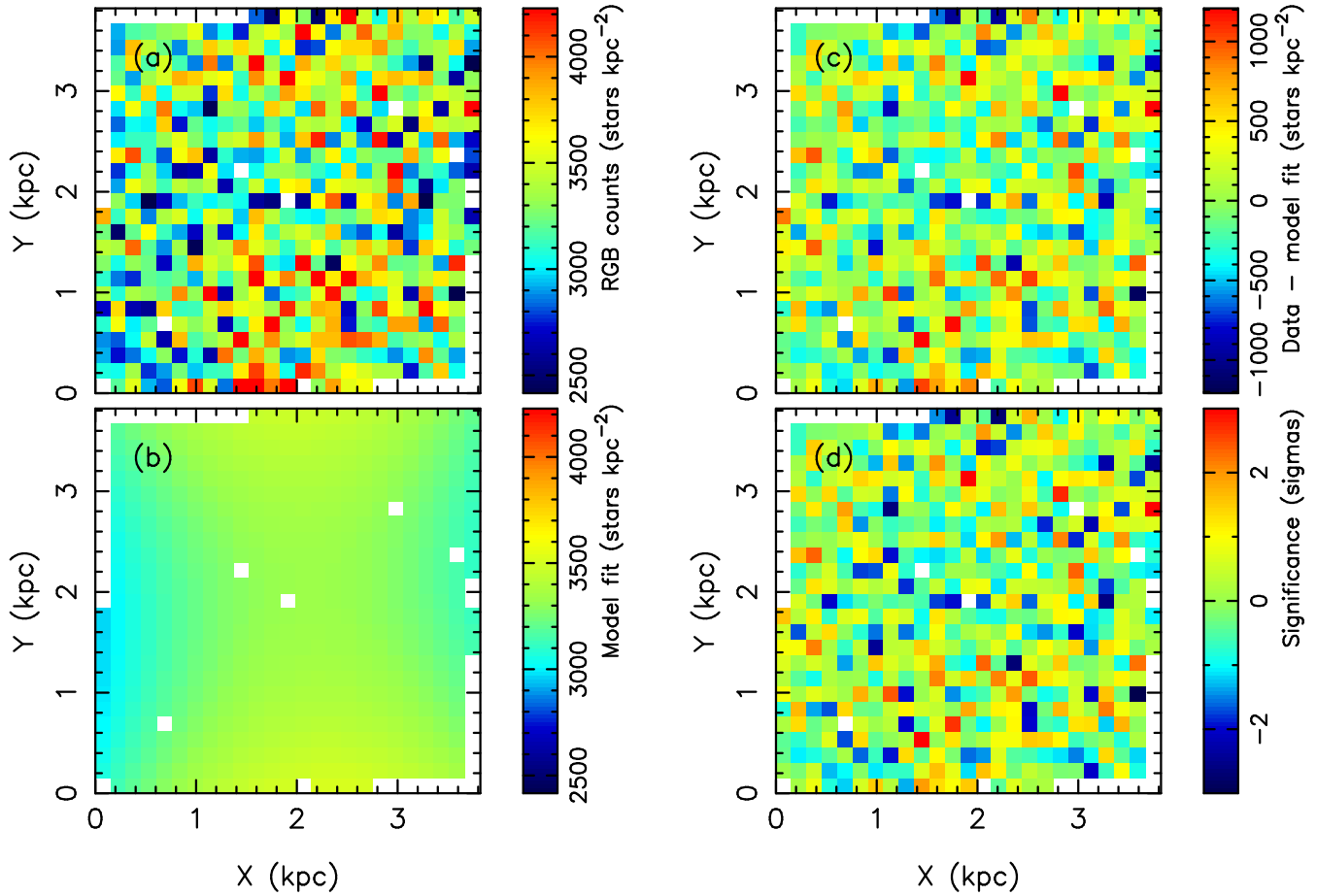


Figure 3. Panel ‘a’ shows the surface density of RGB stars in the ACS field in the coordinate system of Fig. 1, binned into a 25×25 super-pixel array. Clearly, at this distance from the centre of the galaxy, the density is approximately uniform. Fitting a smooth two-dimensional model to the data (panel ‘b’ — fitting details are given in the text) and subtracting shows the small-scale variations apparent in panel ‘c’; the significance of these variations is displayed on panel ‘d’.

Carlo simulations. Artificial stars were added to the frames, which were then reprocessed in the same way as the original data, locating the 50% completeness level of the data at $I \sim 28.8$ and $V \sim 29.7$. The distribution of photometric differences between input and recovered magnitudes as a function of magnitude shows that the photometry is excellent with virtually no bias down to very faint magnitudes; for instance, at $I = 27$ the uncertainty is $\sigma_I \sim 0.1$. We have fitted the R05 uncertainty functions with the following relations:

$$\sigma_V(V) = 2.883 \times 10^{-9} \exp(0.592V + 0.672), \quad (1)$$

$$\sigma_I(I) = 3.029 \times 10^{-7} \exp(0.530I - 1.548), \quad (2)$$

which give a good approximation to the uncertainty estimates for $V < 29$ and $I < 28$. In the analysis below we will assume that the I and V uncertainties are uncorrelated (i.e. with no colour terms, which is a reasonable assumption), so we adopt the above fitting functions to assign uncertainties to the individual stars in the survey. To investigate the properties of the stellar spatial distribution, we select only stars with excellent photometry, i.e., $\sigma_{F606W} < 0.2$ and $\sigma_{F814W} < 0.2$. We further limited the selection to stars with $-0.5 < (V - I)_0 < 4.0$, yielding a catalogue of approximately 43 400 stars.

As well as encompassing stars in the outskirts of NGC 5128, the deep ACS observations also intersect the foreground Galaxy. To estimate the foreground counts, we used the Besançon Galactic population model (Robin et al. 2003) to estimate the foreground contamination. The model predicts 70-80 stars in the range of $I_0 = 21 - 28$ over a field-of-view comparable to that of ACS in the direction of NGC 5128. The right panel of figure 2 shows a typical predicted CMD of the Galaxy foreground stars. The model predicts about 15-20 Galaxy foreground stars with colours and magnitudes similar to those of red giant branch stars at the distance of NGC 5128. This constitutes much less than one per cent of the total number of stellar objects classified as red giant stars in our photometric catalogue, indicating that the foreground contamination is not an issue for the analysis presented below.

Large background galaxies, as well as bright foreground stars cause holes in the stellar distribution map. To correct for this, and for the gap between the two CCDs in the camera, when studying the two-dimensional distribution of stellar density and metallicity, a mask was constructed by choosing suitably large elliptical areas around these problematic regions; in all, 3% of the image was discarded in this manner. Only those stars outside of the masked regions were kept in the final catalogue.

It is well known that the photometric properties of old red giant branch (RGB) stars are linked to their metallicities, offering therefore a way to determine the metallicity distribution of old stellar populations by comparing their colour-magnitude diagrams to RGB tracks. The metallicity of stars on the red clump cannot be estimated however by comparing their photometry to RGB tracks; we therefore imposed a faint cut-off at $M_I < -0.75$ to the catalogue selected above in order to retain only bona-fide RGB stars. This limit corresponds to $I_0 < 27.17$, or $I < 27.38$, where the I -band measurement uncertainty is $\sigma_I = 0.13$. An additional quality cut of $\sigma_V = 0.13$ was imposed to ensure that the V -band measurements were also of good quality, yielding a catalogue

of about 13 300 RGB stars. It is worth mentioning that these magnitude cuts do not exclude metal-rich RGB stars. To estimate the metallicities of the selected RGB stars, we repeat the procedure explained in Mouhcine et al. (2007), interpolating between the models of Vandenberg et al. (2006) of α -enhanced, i.e., $[\alpha/\text{Fe}]=0.3$, RGB stars of mass $0.8 M_\odot$. The models span $-2.014 < [\text{M}/\text{H}] < -0.097$ approximately in steps of 0.1 dex, and are complemented at the metal rich end by two models with $[\text{M}/\text{H}] = 0.0$ and $[\text{M}/\text{H}] = +0.4$. Stars outside of the colour-magnitude range covered by these RGB tracks were flagged and not used in subsequent analysis (i.e., no extrapolation beyond the validity of the models was attempted). At the distance of NGC 5128, the asymptotic giant branch (AGB) bump is found to be located at $I \sim 26.8$ with a dispersion of 0.12 mag (see R05 for more details). The sample of selected bona-fide RGB stars therefore contains AGB bump stars. To examine the effects of this on the estimates of the chemical properties of the population of RGB stars, we constructed two samples by selecting stars brighter than $I = 27.38$ and $I = 26.6$ respectively. The metallicity distribution functions of both samples are found to be almost identical, i.e., the overall shape is unchanged and the changes in the median and/or average metallicities are much smaller than the typical estimate of the metallicity error. This indicates that the presence of AGB bump stars in the selected sample of RGB stars does not bias the results discussed below.

3 ANALYSIS

3.1 Spatial sub-structure

We first perform an analysis of the number density variations over the area of the ACS survey. Panel ‘a’ of Fig. 3 shows the star-count density map in the X, Y CCD coordinate system chosen by R05. We opted to bin the stars in a grid of 25×25 super-pixel, to contain ~ 100 sources (to ensure a signal-to-noise ratio of ~ 10). The star number density has been corrected for the mask, and only super-pixels with a usable surface area larger than 50% were kept. The map appears approximately homogenous, with no obvious gradient. This is not very surprising since the observed field covers a small physical size at the distance of NGC 5128 compared to its projected radial distance. Since we do not have an a-priori model of the large-scale stellar distribution over the targeted field, we fit the observed stellar distribution with a two-dimensional Legendre polynomial function (shown in panel ‘b’), with up to quadratic terms in X and Y including cross-terms (i.e. 6 parameters), which is sufficient to provide a smooth empirical template to compare the data to. The residuals between the data and the best smooth model are shown in panel ‘c’, along with their statistical significance in panel ‘d’, where we have assumed only Poisson noise uncertainties (the effect of the mask is properly accounted for). There appears to be no coherent large-scale structure in the residuals that might indicate the presence of, for instance, streams or shells of stellar debris.

How likely are these small-scale variations about the model of the stellar spatial distribution? A way to quantify the significance of the presence of sub-structure in a survey is to estimate the rms deviation of the data around a smooth model, taking

into account the expected Poisson noise in the model. Bell et al. (2008) proposed the following statistic: $\sigma/\text{total} = \sqrt{\frac{1}{n} \sum_i (D_i - M_i)^2 - \frac{1}{n} \sum_i (M'_i - M_i)^2} / \frac{1}{n} \sum_i D_i$, where n is the number of discrete bins the sample is divided into, D_i are the individual observed counts in those bins, M_i are the model values in the pixels, and M'_i is a Poisson realization of the model with mean M_i . Thus the numerator is the pixel scatter of the data around the model minus the expected scatter in the model, while the denominator was chosen to be the total of the Poisson scatter. This statistic is convenient because it is independent of the choice of binning scale (provided that the substructures are well sampled by the chosen binning scale), and the number of sources in the survey, and furthermore the Poisson noise contribution is removed.

For a bin size ranging from 100 pc to 350 pc, i.e., grids of 42×42 to 12×12 respectively, the fractional rms deviation σ/total varies from 0.04 to 0.02 with probabilities of finding those values of this statistic by chance ranging from 12% to 22%, assuming the smooth model shown in panel ‘b’ of Fig. 3. This clearly indicates that the small-scale deviations of the data around the model shown in Fig. 3 are consistent with what would be expected from Poisson-noise deviations from a smooth model. The stellar populations within the surveyed field are then most likely smoothly distributed at physical scales larger than ~ 100 pc.

This contrasts with what was reported for the two large late-type galaxies where the properties of small-scale substructures have been investigated so far. Bell et al. (2008) found that the fractional rms deviation exceeds $\sigma/\text{total} = 0.4$ in the Galactic halo region probed by the SDSS. For the Milky Way analogue NGC 891, Ibata et al. (2009) have estimated $\sigma/\text{total} = 0.14$ for the extra-planar regions within ~ 10 kpc from the galactic plane, with an extremely small probability of finding this value by chance. This clearly indicates that the spatial distribution of halo stars in both large late-type spiral galaxies is most likely dominated by significantly lumpy components.

The catalogue used in the present analysis integrates stellar populations along the line of sight through the entire halo of the galaxy. The contrast introduced by any substructure will be then reduced, especially in the presence of multiple sub-structures along the probed line of sight. It should then be appreciated that the low fractional rms deviation found here does not necessarily imply that localized spatial over-densities are absent in the halo of NGC 5128. Furthermore, the present survey samples a halo region much smaller than that studied in NGC 891 by Ibata et al. (2009), and a tiny fraction of the halo when compared to the vast region of the Galactic halo sampled by the SDSS data examined in Bell et al. (2008). Wide-field observations covering a representative volume of the outskirts of the galaxy are needed to establish (or to rule out) firmly the predominance of a smooth stellar component at large radii in NGC 5128, and to quantify comprehensively the amount of sub-structures in those regions.

3.2 Metallicity sub-structures

In this section we investigate the properties of the two-dimensional distribution of stellar metallicities over the sur-

veyed region. Given the smaller size of the sample of stars for which we can measure photometric metallicities, we decided to distribute stars in a 12×12 bin grid ($350 \text{ pc} \times 350 \text{ pc}$) to ensure a high signal-to-noise ratio in each super-pixel. The star number density has been corrected for the mask, and we have discarded the few super-pixels where the usable surface area was less than 50%. As in Ibata et al. (2009), we use the median metallicity as a statistic to investigate the spatial variations of stellar populations in the outer regions of the galaxy. This choice presents the advantages of being insensitive to e.g. variations of the population spatial density, holes due to bright stars, etc.

The map of median metallicities estimated in the super-pixels is shown in the upper panel of Fig. 4. The lower panel of the figure shows the map of the uncertainties of median metallicities. The errors on the median metallicity in each super-pixel is estimated by simulating the effects of both the photometric uncertainties on the metallicity estimate for each star belonging to the super-pixel and the sampling uncertainty due to the limited number of stars per super-pixel (see Ibata et al. 2009, for a detailed description). The map shows that the combined random errors on the median metallicities in the super-pixels are of the order of 0.02 – 0.04 dex.

The first clear feature of the median metallicity map is the presence of a large scale gradient over the field, with the average median metallicity decreasing when moving diagonally with increasing Y (i.e., moving from the West to the East). A second striking feature of the median metallicity map is that the pixel-to-pixel variations are significantly larger than the random errors. Note that while we notice the presence of numerous super-pixels dominated by stellar populations with lower median metallicities, i.e., $[M/H] \lesssim -0.7$, than that of the overall stellar population, i.e., $[M/H] \sim -0.6$, it appears however that metal-rich, i.e., $[M/H] \gtrsim -0.5$, super-pixels are rare. How likely are those small-scale variations about a large-scale smooth model of the median metallicity distribution?

To represent the large-scale spatial distribution of median metallicities, we fitted the observed distribution with a two-dimensional Legendre polynomial (up to order 3 in both spatial directions, i.e., 10 parameters). The fit is shown in the top panel of Fig. 5, and exhibits clearly a large-scale median metallicity gradient. The middle panel of Fig. 5 shows the difference between the map of median metallicities and the best smooth model, while the lower panel shows the map of the significance levels of these differences. The lower panel of the figure shows clearly the presence of localized variations at the $3\text{-}5\sigma$ level in the median metallicity map, occurring on the scale of a super-pixel or a few super-pixels, and distributed over the field. When comparing the significance map of the deviations of the median metallicity map about the best smooth model to the maps of the spatial density distribution and the deviation about the best smooth model (see Fig. 3), we notice that the small-scale sub-structures in the median metallicity map are not systematically associated to small-scale stellar density sub-structures. As already discussed in detail in our study of NGC 891, the number density of stars required to cause statistically significant deviations about a smooth median metallicity map is rather small, causing only a modest enhancement in the stellar distribution that is much harder to detect from its density

contrast. The stellar number density needed to cause a deviant super-pixel in the median metallicity map depends on the shape of the metallicity distribution functions of both the smoothly-distributed population and the super-imposed sub-structures, but in broad terms an additional stellar population numbering 10–15 per cent of the smooth population could induce a ~ 0.1 dex metallicity variation (Ibata et al. 2009). While this mass fraction of the super-imposed population is of the order of the change in density over a typical super-pixel, the induced change in the median metallicity of the super-pixels is many times larger than the typical errors on the estimate of the median metallicity (see the lower panel of Fig. 4). It is then not surprising that sub-structures detected in the median metallicity map are not inducing significant deviations in the number density map.

The distribution function of the statistical significance of the variations about the best smooth model of the median metallicities map is shown in Fig. 6. The dashed line shows a fitted Gaussian of dispersion equal to 1.58. The probability of finding such a large dispersion by chance (we expect unit dispersion if the uncertainties have been correctly estimated), given the large number of bins, is smaller than 0.1%. This strongly indicates that the variations about the best smooth model of the spatial distribution of median metallicities are significantly larger than expected for a population where the median metallicity varies spatially in a smooth manner.

Perhaps the simplest explanation of these large deviations is that we have underestimated the uncertainties in the median metallicity by 30–50%. This would require that the photometric errors reported by R05 to be underestimated by a similar factor. In our study of NGC 891 we were able to verify our uncertainty estimates by comparing measurements in overlapping fields. Unfortunately, we do not have the necessary complementary data to perform a similar check here. Although we cannot dismiss this possibility, experience from our NGC 891 study (and other projects) suggests that artificial star simulations give reliable uncertainty estimates.

The large pixel-to-pixel variations reported in the median metallicity map are unlikely to result from errors in the zero-point over the ACS field. To induce the observed small-scale metallicity changes, large variations in the zero point (of the order of 0.1 mag or more) are required, which is extremely unlikely for the very stable instrument that the ACS is.

Could the large-scale metallicity gradient and the small-scale chemical substructures we have uncovered be due to systematic biases? To convert the RGB photometric properties into metallicities, we have had to assume that the stellar populations dominating the surveyed field are uniformly old. Due to the so-called age-metallicity degeneracy, a red RGB star can be either more chemically evolved than a bluer one or older. In the interpolation procedure, we have assumed a single old age for all the stars, which may introduce a bias of up to 0.1 dex, if the age is ~ 4 Gyr younger (e.g. Rejkuba et al. 2005).

The AGB stars are known to be efficient tracers of intermediate age (1–6 Gyr) stellar populations (Mouhcine & Lançon 2002; Marigo & Girardi 2007). The abundance of AGB stars normalized to RGB stars, which are tracing predominantly older populations, is a good in-

dicator of a stellar population age (e.g. Frogel et al. 1990). The map of the ratio of AGB stars, selected as stars with $22.0 < I_o < 23.5$ and $1.5 < (V - I)_o < 3.0$, and all other quality criteria identical to the RGB sample summarized in §2, to stars in the brightest one magnitude of the RGB is shown in Fig. 7. The spatial distribution of the AGB to RGB ratio is fairly smooth, with no apparent spatial gradient. This suggests the absence of an AGB gradient and then most likely the absence of an age gradient across the observed field. Furthermore, no enhancements of AGB stars relative to RGB stars are associated to any of the super-pixels that are deviants from a smooth model of the median metallicity map by more than 3σ . Interestingly, the typical AGB to RGB ratio, i.e., $\lesssim 0.2$, is consistent with an old stellar population (Mould 2005). The pixel-to-pixel variations of the AGB-to-RGB ratio are significantly smaller than what is required for the pixel-to-pixel variations of the median metallicities to be due only to age differences: to account for the $\gtrsim 0.15$ dex variations in median metallicity about the best smooth model for the most deviant super-pixels (i.e., $\pm 3\sigma$ or more) as a result of age differences, the stellar populations of those super-pixels have to be dominated by $\lesssim 6$ Gyr stars, which is not supported by the morphology of the colour-magnitude diagram (see Rejkuba et al. 2005, for a detailed discussion).

The localized median metallicity variations are also unlikely to result from the effects of small-scale structures in the foreground Galactic inter-stellar medium. Following Ibata et al. (2009), by using the reasonable assumption that reddening variations scale approximately linearly with mean reddening, we expect less than a couple hundredths of a magnitude scatter at most in colour excess from foreground dust. For the small-scale metallicity variations to be due solely to variation in foreground extinction, the required offset in colour excess are either much larger than the expected scatter, or, more problematically, negative in the case for deviant metal-poor super-pixels. Small angular scale variations in foreground dust are therefore unlikely to contribute significantly to the observed small-scale variations in median metallicity.

We conclude that there is no evidence for systematic biases affecting the measure of stellar metallicities. So, under the assumption that the photometric uncertainties have been well estimated, we conclude that the statistically significant small-scale variations in the median metallicities of the stellar populations are present in the targeted halo field. To highlight the differences between the detected small-scale chemical inhomogeneities, Fig. 8 shows the CMDs of all stellar objects populating a metal-poor super-pixel, i.e., with a median metallicity of $[M/H]=-0.77$, and a metal-rich super-pixel, i.e., with a median metallicity of $[M/H]=-0.47$, located at $(X/\text{kpc}=1.75, Y/\text{kpc}=3.00)$ and $(X/\text{kpc}=2.40, Y/\text{kpc}=0.48)$ respectively. Fiducials of RGB sequences for Galactic globular clusters spanning a wide range of metallicities and shifted to the distance of NGC 5128 are overplotted. The stellar populations occupying both super-pixels appear to be different. A significant fraction of bright RGB stars populating the metal-poor super-pixel exhibit photometric properties consistent with metallicities in the range of $[Fe/H]=-2.2$ and -1.3 . Such metal-poor stars are absent in the metal-rich super-pixel. Furthermore, the reddest stars in the metal-rich super-pixel extend clearly to higher metal-

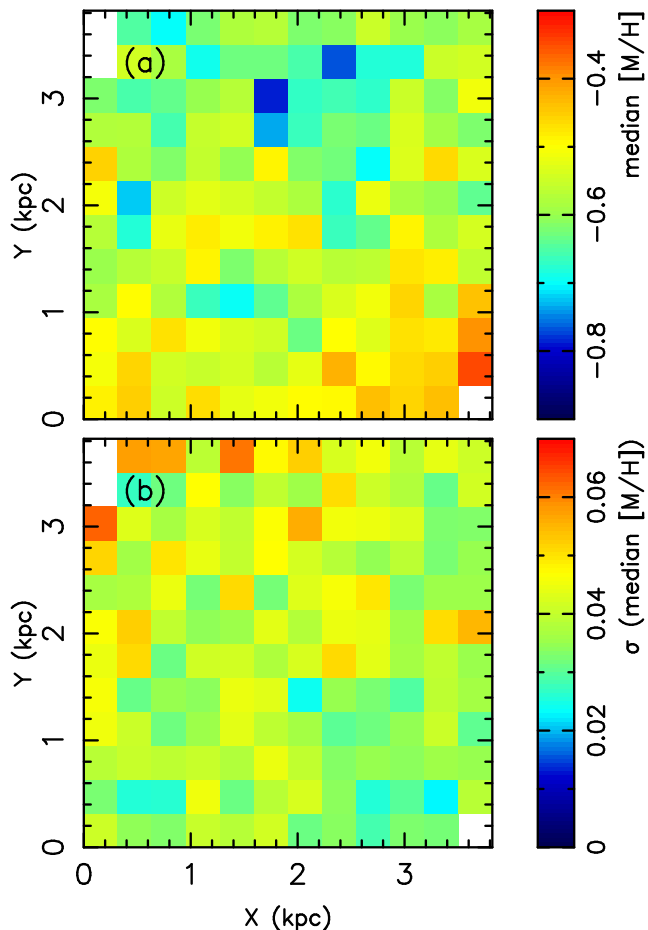


Figure 4. Panel ‘a’ displays the median metallicity calculated in each of the spatial super-pixels. A slight gradient is apparent, with the top left-hand corner being more metal-poor than the bottom right. The corresponding uncertainties, calculated from Monte-Carlo simulations accounting for both the photon noise and the sampling errors, are shown on the panel ‘b’.

licities than those occupying the metal-poor super-pixel. The stellar population differences between the localized substructures in the median metallicity spatial distribution would suggest that the survey has revealed the presence of inhomogeneities that have not yet been fully blended into the smooth halo.

4 DISCUSSION

The metallicity distribution function of the stellar populations in the outer regions of NGC 5128 has been determined over an extended range of radial distances, 10-40 kpc (Harris et al. 1999; Harris & Harris 2002; Rejkuba et al. 2005). The overall shape, mean metallicity, metallicity dispersion, fraction of metal-poor stars, are found to be strikingly similar (Rejkuba et al. 2005) over these fields. This indicates that the metallicity gradient present within the field at ~ 40 kpc (see Fig. 5) could not be associated to a large-scale metallicity gradient, as it would lead to metallicities significantly higher than observed if extrapolated inward. The most likely explanation is that the median stellar

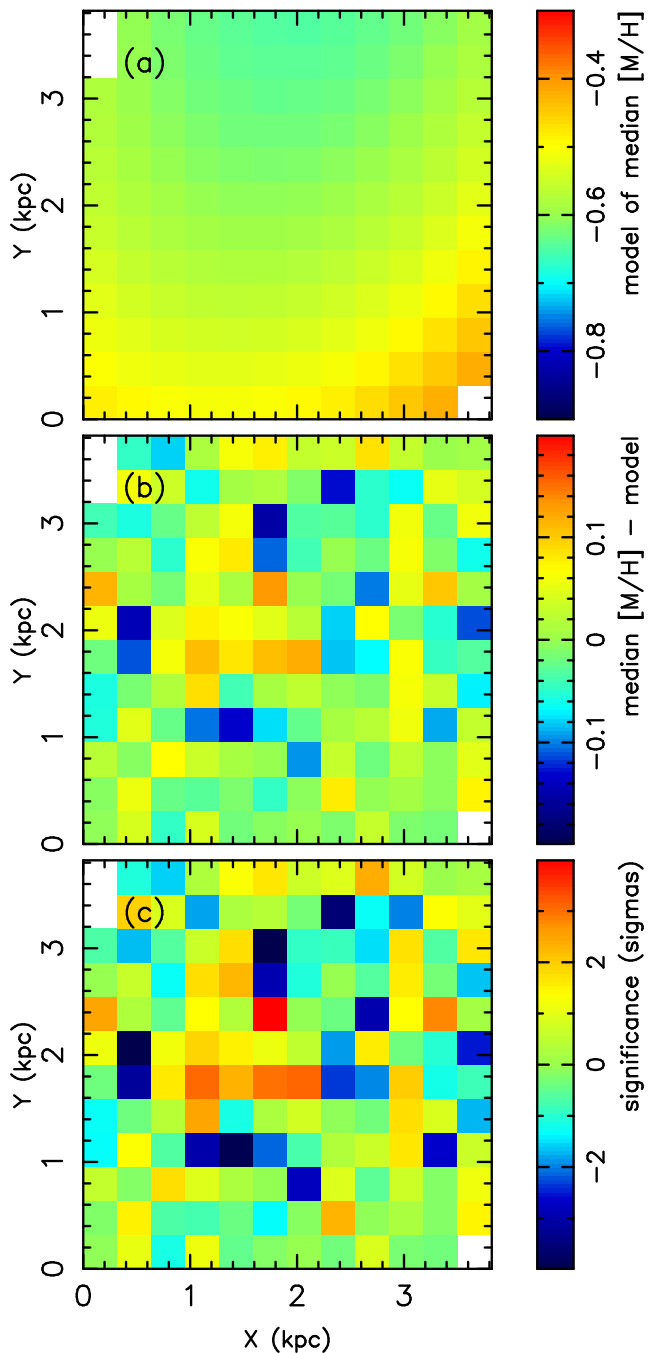


Figure 5. A two-dimensional polynomial model fit to the median metallicity map (panel ‘a’ of Fig. 4) is shown in panel ‘a’. The residuals between the data and this model are displayed in panel ‘b’. Using the uncertainty estimates on the metallicity metallicity from panel ‘b’ of Fig. 4, the statistical significance levels of the metallicity variations are shown in panel ‘c’.

metallicity gradient present within the ACS halo field is related to chemical inhomogeneities present locally.

Using the predictions of a Λ -cold dark matter semi-analytical galaxy formation model, and by summing the total star formation occurring over all the progenitors, Beasley et al. (2003) computed the metallicity distribution function of spheroid stars of early-type galaxies comparable

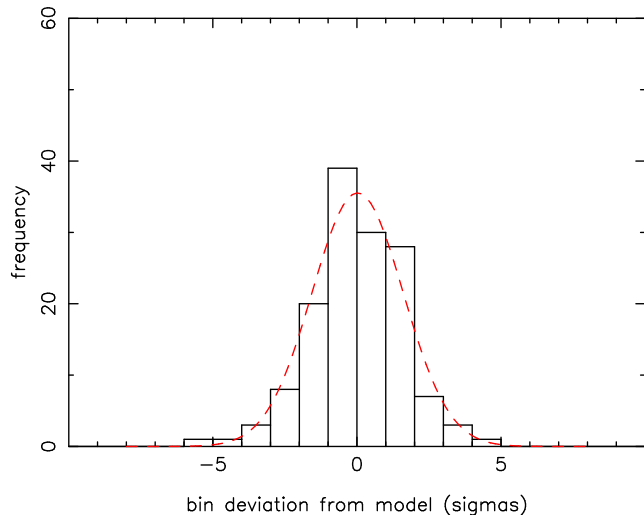


Figure 6. The distribution of statistical significance of the deviations from the best smooth model of the median metallicity map shown in the top panel of Fig. 5. The Gaussian model fit superimposed on this distribution has a dispersion of 1.58. The distribution of significance levels has an extremely small probability of being drawn by chance from a Gaussian distribution of unit dispersion.

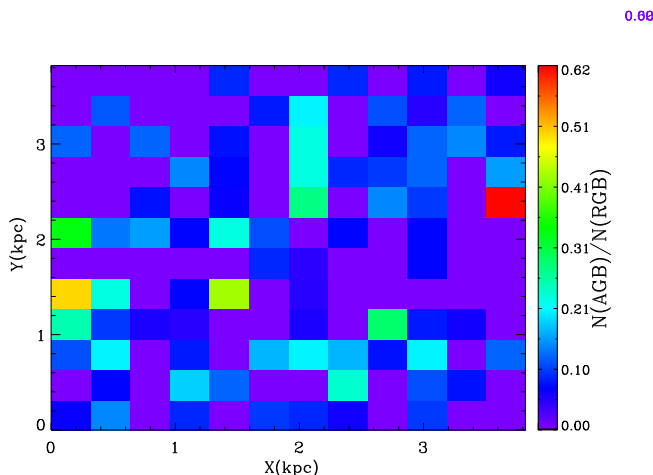


Figure 7. The spatial distribution of the ratio of AGB stars to RGB stars over the ACS field.

in luminosity and environment to NGC 5128. Despite some differences, the predicted metallicity distribution function resembles qualitatively the observed distribution function of stellar metallicities in the outer regions of NGC 5128, i.e., mean metallicity, metal-rich end cut-off, and extent of the metal-poor tail (see Rejkuba et al. 2005). This broad agreement suggests that the stellar populations in the outer regions of NGC 5128 could have been assembled in a hierarchical fashion. If this is indeed the case, one can expect to find the presence of chemical sub-structures caused by the remnants of the disruption of the predicted large populations of sub-halos orbiting around massive galaxies.

The localised chemical inhomogeneities could be in principle potential candidate satellites or remnants of past ac-

cretion events. Upon inspecting the stacked ACS image visually, none of the strongly deviant super-pixels shows any plausible stellar concentration, although clear RGB sequences are detected for all of them, apart from the super-pixel at ($X \sim 1.8$ kpc, $Y \sim 3$ kpc) which contains the faint, old, and metal-poor extended globular cluster reported in Mouhcine et al. (2010b). The extended nature and the low luminosity of that globular cluster become very important when considered in light of the emerging consensus that extended clusters are formed preferentially in low mass galaxies (e.g. Elmegreen 2008; Da Costa et al. 2009). In M31, all but one extended globular cluster in the outer halo, i.e., at projected distances larger than 30 kpc, are found to be projected onto stellar substructures or are members of a cluster overdensity (Mackey et al. 2010), supporting the scenario where this class of globular clusters originate in low mass systems.

The properties (luminosity, surface brightness, size, central concentration) of the globular cluster found in the halo field resemble in every way one those of the faint and extended globular clusters populating the Milky Way outer halo (Mouhcine et al. 2010b). This suggests that the extended cluster in the targeted field could have been formed in a similar environment as its Galactic counterparts, and experienced potentially a similar dynamical history. Strong evidence is accumulating that extended and faint globular clusters in the outer Galactic halo, i.e., the so-called young halo globular clusters, were associated with dwarf galaxies that have since disrupted (e.g. Zinn 1993; Mackey & Gilmore 2004; Forbes & Bridges 2010). Mackey et al. (2010) have argued that the vast majority of globular clusters in the outer halo of M31 are most likely associated with tidal debris features observed in those regions, thus strongly supporting the scenario where the outer globular cluster system of M31 has been built up via the accretion of satellite host galaxies. It is then tempting to suggest that the extended faint cluster in the surveyed halo field in NGC 5128 could have originated in a now disrupted dwarf galaxy. Interestingly, the median metallicity of the diffuse stellar population within the super-pixel containing the extended faint cluster is comparable to those measured for metal-poor super-pixels deviants at the $3-4\sigma$ levels in the observed halo field, i.e., $[M/H] \sim -0.75$, suggesting that the stellar populations dominating the metal-poor super-pixels could be sharing the same origin. Put together, these properties provide circumstantial evidence that the chemical inhomogeneities detected in the observed field could be related to the disruption of low mass satellites.

The restricted spatial extent of the present survey limits however our ability to investigate the large-scale distribution of the chemical sub-structures, to quantify the degree of spatial sub-structures in the halo of the galaxy, to search for signs of the disruption of the hypothetical progenitor(s) of the detected chemical sub-structures. Extending the survey of the outer regions of NGC 5128 should be undertaken to tackle comprehensively these questions. When compared to the properties of sub-structures in the outskirts of late-type galaxies, it will be possible to constrain the assembly histories of galactic halos as a function of galaxy e.g. morphology, type, and mass.

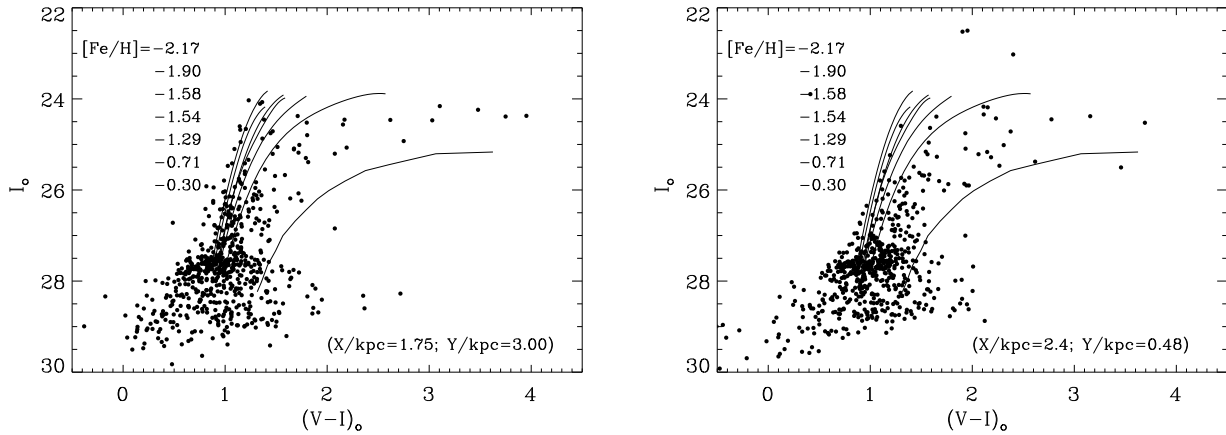


Figure 8. CMDs of stars populating two super-pixels with their respective positions indicated in each panel. The left panel shows the CMD of the most metal-poor super-pixel in the map shown in Fig. 4 with a median metallicity of $[M/H]=-0.77$, while the right panel shows the CMD of a typical metal-rich super-pixel with a median metallicity of $[M/H]=-0.41$. Note that the median metallicity for the whole field is $[M/H]=-0.53$. Shown also as solid lines are the red giant sequences of the indicated Galactic globular clusters from Da Costa & Armandroff (1990) assuming an intrinsic distance modulus for NGC 5128 of 27.9. It is clear that the metal-poor side of the red giant branch is much more populated in the case of the metal-poor spatial super-pixel than for the metal-rich one.

5 SUMMARY & CONCLUSIONS

To make the first attempt to quantify the degree of substructure in the outer regions of elliptical galaxies, we have undertaken a structural and chemical analysis of the stellar content of a $3.8 \text{ kpc} \times 3.8 \text{ kpc}$ halo field situated $\sim 38 \text{ kpc}$ from the centre of the nearest giant elliptical galaxy NGC 5128. The very deep colour-magnitude diagram of the stellar populations used in the analysis reaches the red clump.

Comparing the observed stellar number density map of halo stars to smooth models, we find no statistically significant evidence for the presence of spatial density variations. Deviations from the smooth models, quantified using the rms deviation of the data around the best fit model are consistent with what would be expected from Poisson-noise deviations in a smooth model. The measured statistics appears to suggest the presence of a smooth stellar halo component at spatial scales larger than $\sim 100 \text{ pc}$ in the region probed by the present survey.

Estimating metallicities of RGB stars from their optical photometry, we investigated the spatial distribution of stellar metallicities. On top of a smoothly distributed large-scale map, we detect the presence of small-scale substructures in the median metallicity across the surveyed field. Although the absolute median metallicity variations are relatively modest, i.e., ranging from ~ 0.08 to ~ 0.2 dex, they are nevertheless statistically significant. Those small-scale chemical sub-structures do not appear to be associated with any statistically significant stellar spatial density variations. We argue that these subtle small-scale metallicity variations are related to accretions of low mass systems.

REFERENCES

- Abadi M. G., Navarro J. F., Steinmetz M., 2006, *Mon. Not. R. Astron. Soc.*, 365, 747
- Ashman K. M., & Zepf S. E., 1992, *Astrophys. J.*, 384, 50
- Beasley M. A., Harris W. E., Harris G. L. H., Forbes D. A., 2003, *Mon. Not. R. Astron. Soc.*, 340, 341
- Bell E. F., et al., 2008, *Astrophys. J.*, 680, 295
- Belokurov, V., et al., 2007, *Astrophys. J.*, 654, 897
- Burstein D., Heiles C., 1982, *Astronomical Journal*, 87, 1165
- Côté P., Marzke R. O., West M. J., 1998, *Astrophys. J.*, 501, 554
- Da Costa G. S., Armandroff T. E., 1990, *Astron. J.*, 100, 162
- Da Costa G. S., Grebel E. K., Jerjen H., Rejkuba M., Sarina M. E., 2009, *Astron. J.*, 137
- Elmegreen B. G., 2008, *Astrophys. J.*, 672, 1006
- Forbes D. A., & Bridges T., 2010, *Mon. Not. R. Astron. Soc.*, 404, 1203
- Frogel J. A., Mould J., Blanco V. M., 1990, *Astrophys. J.*, 352, 96
- Grillmair C. J. Dionatos, O. 2006, *Astrophys. J.*, 643, L17
- Grillmair C. J., 2006, *Astrophys. J.*, 693, 1118
- Harris W.E., Pritchett C. J., McClure R. D., 1995, *Astrophys. J.*, 441, 120
- Harris G.L.H., Harris, W.E., & Poole, G.B., 1999, *Astron. J.*, 117, 855
- Harris G.L.H., & Harris W.E., 2000, *Astron. J.*, 120, 2423
- Harris W.E., & Harris, G.L.H. 2002, *Astron. J.*, 123, 3108
- Harris, G. L. H., et al., 2009, *arXiv:0911.3180*
- Ibata R., Chapman S., Ferguson A. M. N., Lewis G., Irwin M., Tanvir N., 2005, *ApJ*, 634, 287
- Ibata R., Irwin M., Lewis G., Ferguson A. M. N., Tanvir N., 2001, *Nature*, 412, 49
- Ibata R., Martin N. F., Irwin M., Chapman S., Ferguson A. M. N., Lewis G. F., McConnachie A. W., 2007, *ApJ*, 671, 1591
- Ibata R. A., Gilmore G., Irwin M. J., 1994, *Nature*, 370, 194
- Ibata R. A., Irwin M. J., Lewis G. F., Ferguson A. M. N., Tanvir N., 2003, *MNRAS*, 340, L21
- Ibata, R., Mouhcine M., Rejkuba M., 2009, *Mon. Not. R.*

- Astron. Soc., 395, 126
- Larson R. B., 1974, *Mon. Not. R. Astron. Soc.*, 166, 585
- Malin, D. F., Quinn, P. J., Graham, J. A. 1983, *ApJ*, 272, L5
- Majewski S. R., et al., 2003, *Astrophys. J.*, 599, 1082
- Marigo P., & Girardi L., 2007, *A&A*, 469, 239
- Mackey A. D., & Gilmore, G. F., 2004, *Mon. Not. R. Astron. Soc.*, 355, 504
- Mackey A. D., et al., 2010, *Astrophys. J. Letter*, in press
- Marleau et al. 2000, *Astron. J.*, 120, 1779
- Mouhcine M., Lançon A., 2002, *A&A*, 393, 149
- Mouhcine, M., Rejkuba M., Ibata R., 2007, *Mon. Not. R. Astron. Soc.*, 381, 873
- Mouhcine, Ibata R., Rejkuba M., 2010, *Astrophys. J. Let.*,
- Mouhcine, M., Harris W. E., Ibata R., Rejkuba M., 2010, *Mon. Not. R. Astron. Soc.*,
- Mould, J. R., et al. 2000, *Astrophys. J.*, 536, 266
- Mould J., 2005, *Astron. J.*, 129, 698
- Newberg H. J., et al. 2002, *Astrophys. J.*, 569, 245
- Odenkirchen M., et al., *Astrophys. J.*, 548, 165
- Peng E. W., Ford H. C., Freeman K. C., 2004, *Astrophys. J.*, 602, 685
- Rejkuba M., Minniti D., Silva D. R., Bedding T. R., 2001, *A&A*, 379, 781
- Rejkuba M., Minniti D., Courbin F., Silva D. R., 2002, *Astrophys. J.*, 564, 688
- Rejkuba M., Minniti D., Silva D. R., Bedding T. R., 2003, *A&A*, 411, 351
- Rejkuba M., Gregio L., Harris W. E., Harris G. L. H., Peng E. W., 2005, *Astrophys. J.*, 63, 262
- Robin A., Reylé C., Derrière S., & Picaud S., 2003, *A&A*, 409, 523
- Schlegel D. J., Finkbeiner D. P., Davis M., 1998, *Astrophys. J.*, 525, 500
- Soria R., et al., 1996, *Astrophys. J.*, 465, 79
- Stetson P. B., 1994, *Pub. Astron. Soc. Pac.*, 106, 250
- Stickel M., van der Hulst J. M., van Gorkom J. H., Schiminovich D., Carilli C. L. 2004, *A&A*, 415, 95
- Toomre A., 1977, *ARA&A*, 15, 437
- VandenBerg D. A., Bergbusch P. A., Dowler P. D., Swenson F., 2006, *Astrophys. J. Suppl.*, 162, 375
- Yanny B., et al., 2000, *Astrophys. J.*, 540, 825
- Yanny B., et al., 2003, *Astrophys. J.*, 588, 824
- Woodley et al. 2010, *ApJ*, 708 1335
- Zinn R., 1993, in Smith G. H., Brodie J. P., eds. *ASP Conf. Ser. 48. The Globular Cluster-Galaxy Connection*. *Astron Soc. Pac. San Francisco*, p. 38
- Zolotov A., Willman B., Brooks A. M., Governato F., Brook C. B., Hogg, D. W., Quinn T., Stinson G., *Astrophys. J.*, 702, 1058